LEGIBILITY NOTICE

A major purpose of the Technical Information Center is to provide the broadest dissemination possible of information contained in DOE's Research and Development Reports to business, industry, the academic community, and federal, state and local governments.

Although portions of this report are not reproducible, it is being made available in microfiche to facilitate the availability of those parts of the document which are legible.

3

LA-UR -90-419

Los Alamos National Laboratory is operated by the University of California for the United States Department of Energy under contract W-7405-ENG-36

LA-UR--90-419

DE90 007623

TITLE **LASER-PRODUCED PLASMAS IN MEDICINE**

AUTHOR(S) Steven J. Gitomer and Roger D. Jones

SUBMITTED TO SPIE - International Society of Optical Engineering - Biomedical Optics '90, 14-19 January 1990, Los Angeles, CA - Conference 1202, Laser-Tissue Interaction

DISCLAIMER

Los Alamos Los Alamos National Laboratory
Los Alamos, New Mexico 87545

SPIE - International Society of Optical Engineering - Biomedical Optics '90
14-19 January 1990, Los Angeles, CA - Conference 1202, Laser-Tissue Interaction 1202-13

LASER-PRODUCED PLASMAS IN MEDICINE*

S. J. Gitomer & R. D. Jones

Applied Theoretical Physics Division, Los Alamos National Laboratory, Los Alamos NM 87545 USA

ABSTRACT

The laser has found numerous applications in medicine, beginning with uses in ophthalmology in the 1960's. Today, lasers are used in tissue cutting, blood coagulation, photo-dynamic cancer therapy, arterial plaque removal, dental drilling, etc. In this paper, we examine those areas of laser medicine in which plasmas (ionized gases) are produced. In fact, the presence of a plasma is essential for the application at hand to succeed. We consider examples of the plasmas produced in ophthalmology (e.g. lens membrane destruction following cataract surgery), in urology and gastroenterology (e.g. kidney and gall stone ablation and fragmentation) and in cardiology and vascular surgery (e.g. laser ablation and removal of fibro-fatty and calcified arterial plaque). Experimental data are presented along with some results from computer simulations of the phenomena. Comments on future directions in these areas are included.

I. INTRODUCTION

The cover of the journal stated "Zap Goes the Kidney Stone" and the article title [1] claimed that "Plasma Physics Breaks Stones." Thus we were first alerted to the fact that plasmas were being beneficially used in laser medicine. The article continued that μs duration dye laser pulses, introduced into the body via a fiber optic delivery system were successfully fragmenting kidney stones in patients. From that first article to the work presented below, our interest in laser produced plasmas in medicine has grown.

It is well known that lasers have been utilized in medicine for many years. Lasers were used first in ophthalmology and dermatology, beginning in the early 1960's, shortly following the laser's invention. Today's applications of the laser in medicine are diverse - including tissue cutting and welding, blood coagulation, photo-dynamic cancer therapy, arterial plaque removal, Port-wine-stain (dermatology) removal, dental drilling, etc. It is not so well known that there are a few areas of laser medicine in which a plasma (ionized gas) plays a central role. It is the purpose of this paper to introduce the reader to the present day applications of laser produced plasmas in medicine and to speculate on the future of this phenomena.

When a laser is incident upon a material, a number of effects can be observed depending upon the laser intensity, pulse duration and wavelength. Considering intensity alone, for the moment, we'd expect that as intensity is increased, we would first observe heating of the material, followed by melting and then vaporization. At still higher laser intensities, we'd expect the breaking of chemical bonds and finally ionization. A simple energy density ordering for these phenomena is shown in Fig. I-1, using H_2O as a sample material. In the Figure, $\rho(P_n,T_n)$ is the mass density (gm/cm^3) at pressure P_n and temperature T_n while the symbol ε denotes the energy in eV to which the material is being raised (ε is presumed to be of the order of unity). Thus, a laser deposited energy density of 334 J/cm^3 would be needed to melt ice (mass density 1 gm/cm^3) while 2258 J/cm^3 would be needed to vaporize water, etc. Depending upon the mass density and the final energy, vaporization, bond breaking and ionization may all be competing processes. When one deals with biological tissue, each of the foregoing stages from heating to ionization may be observed.

The diversity of medical applications of lasers can be more fully appreciated by reference to the "Medical laser interaction map" taken from the work of J.-L. Boulnois [2]. This map is displayed in Fig. I-2. Power density (or irradiance or intensity in $Watts/cm^2$) is plotted versus interaction time (in seconds). Diagonal lines denote constant laser fluences in $Joules/cm^2$. The various interaction regimes from thermal and photochemical through photoablative and electromechanical occur for a limited range of fluences (between about 10 and 1000 J/cm^2). The interaction regimes can be roughly separated by the time duration of the laser pulse. Long pulses correspond to the thermal and photochemical regimes while short pulses correspond to the photoablative and electromechanical regimes. Boulnois defines these interaction regimes as follows: (1) thermal - conversion of electromagnetic energy into thermal energy; (2) photochemical - spectrally sensitive chemicals (chromophores) injected locally, activated by absorption of laser photons; (3) photoablative - direct photodissociation of intramolecular bonds by absorption of photons; and (4) electromechani-

GITOMER

cal - thermionic emission or multiphoton production of free electrons leading to dielectric breakdown and plasma production. We will concern ourselves in the remainder of this paper with the electromechanical regime - the one in which a plasma is produced.

It is worthwhile to note that non-laser produced plasmas appear in biology and medicine. In paleobiology, for example, it has been speculated that amino acids, essential to life, could have been formed in Earth's primordial atmosphere by lightning discharges. Thus life may owe its origin to a plasma process. In addition, RF electric discharges have been used in dermatology to remove skin growths, in general surgery to remove diseased tissue (the technique is commonly referred to as *electrocautery*), and in urology to fragment kidney stones (the technique is known as *electrohydraulic lithotripsy*). It is even possible that medical research will yet investigate a plasma (liquid part of the blood) plasma (ionized gas)! We will concern ourselves here, however, with the work on plasmas in medicine by limiting our scope to those plasmas which are produced by lasers.

II. LASER PRODUCED PLASMAS IN OPHTHALMOLOGY

Almost since the invention of the laser in the early 1960's, lasers have been used in a wide range of ophthalmic procedures. Laser produced plasmas in ophthalmology, however, are more recent, appearing to date from the work of Krasnov [3], Bass et al. [4], van der Zypen et al. [5] and Aron-Rosa et al. [6]. These researchers used short pulsed ruby, dye or Nd:YAG lasers (tens of ns to one μs laser pulse duration, tens of mJ laser energy, tens of μm laser spot diameter). The laser light was focused by an external lens upon structures within the eye, producing a plasma. The researchers [5,6] hypothesized that following the plasma production, shock waves were produced which caused the observed tissue destruction. The ophthalmologic procedures in which plasmas are produced include: (1) shattering of the opaque posterior capsule (capsulotomy) which remains in the eye following cataract removal and artificial lens implantation [6]; (2) puncturing an opening in the iris (iridotomy) to reduce intraocular pressure in glaucoma [3,4,7]; and (3) destroying opaque strands within the vitreous humor [8]. For reference, we show in Fig. II-1 a diagram of the human eye [9]. The posterior capsule refers to the membrane forming the lens surface nearest to the vitreous. The iris and the vitreous are also shown. The term *photodisruption* has become accepted parlance among ophthalmologists for the effect of the laser in the above mentioned procedures.

Following the research of van der Zypen and Aron-Rosa, work was commenced on understanding the physical phenomena involved in the laser interaction. Questions concerning the characteristics of the plasma produced, the efficacy of plasma shielding, the utility of concomitant shock or acoustic waves, the short term and long term damage risk to nearby tissue, etc. were addressed. Research was concentrated on breakdown and subsequent phenomena for lasers focused in liquid media (saline, water, vitreous, etc). Let us consider the phenomena studied to date, both during and following the laser pulse, and their effects.

A. Phenomena for $0 \leq t \leq \tau_{laser}$

The physical phenomena which are likely taking place in the laser interaction are the following [10]. Free electrons are initially produced either by multiphoton effects or via thermionic emission. These electrons grow in number and are themselves accelerated in the laser field to lead to avalance breakdown. The resulting plasma then grows until it achieves dimensions comparable to the focal spot diameter. The plasma continues to grow and absorb the laser light which impinges upon the focal volume, now by inverse bremsstrahlung absorption [11].

The optical breakdown aspect of the laser pulse focused in saline was studied by a number of researchers [10], [12] - [16]. Saline is used as a model material for various kinds of tissue. Both Q-switched and mode locked Nd:YAG lasers were employed. It was noted that "Optical breakdown with plasma formation was detected as a visible spark to a dark adapted observer" [10]. The results of the breakdown threshold studies for the two different laser types are given in Table 1. It is worthwhile to note that the thresholds fall near or within the electromechanical region defined by Boulnois [2] as shown in Figure 2. Variations in breakdown threshold between groups using similar lasers appear to be due to important differences in laser pulse shape and/or bubbles and impurities in the saline medium.

Plasma luminescence or lifetime has been studied experimentally by several groups [14], [17], [18] & [19]. Time resolution was obtained in these experiments with photomultipliers, fast photodiodes and streak cameras. The signals were characterized by fast initial risetimes followed by slower decays. For the subnanosecond laser pulses [19], the peak luminescence lags the peak of the laser pulse. For the nanosecond Nd:YAG laser pulses [14], [18], [19], both peaks coincide. Results for ruby [17] show the peak emission lagging the peak of the laser pulse by 15 ns. The reason

for the inconsistency between ruby and Nd:YAG lasers is not understood. Bremsstrahlung emission, whose strength at any time should scale as the electron density squared, appears to be responsible for the observed luminescence [19]. Docchio [19] has also shown that both electron-ion recombination and electron-neutral attachment are important processes in the decay of the luminescence radiation.

The temporal and spatial evolution of the breakdown plasma has also been studied by Docchio et al. [18] & [20]. Experiments in distilled water, using 12 ns Nd:YAG laser pulses, were diagnosed with a streak camera and a photomultiplier. It was found that following breakdown, the plasma grows in time as a cylindrical column, toward the laser (away from the focal point). The portion of the plasma nearer to the laser, shields the plasma closer to the focal point causing the luminescence signal near focus to decay. The longest duration luminescence signal occurs for the plasma formed nearest to the laser. Using a moving breakdown model augmented by a distributed plasma attenuation of the laser beam, the authors have fit rather well the spatial and temporal evolution of the plasma luminescence in the nanosecond regime.

B. Phenomena for $t > \tau_{laser}$

Following the end of the laser pulse, the plasma cools and expands. The physical phenomena present were first elucidated clearly by Felix and Ellis [21], although much work on laser produced plasmas in liquids came before [17,22,23]. First there is the emission of a shock wave into the surrounding liquid medium. The shock which propagates initially at supersonic speed slows to sonic within the first 100 μm [14,16] (see Fig. II-2). Measurements of the shock wave and subsequent acoustic transient into which the shock wave evolves have been made using a pump-probe technique [14,16,24] and using high-speed photography [25]. This work shows that the propagation far into the liquid medium of the acoustic transient is at the local sound speed (roughly 1500 m/s in water). Measurements and analysis [using work from Ref. 26] by Vogel and Lauterborn [24] have shown that as much as 3.5% of the incident laser pulse energy is carried away in the acoustic transient for a 4 mJ laser pulse.

The plasma filled cavity continues to expand and cool, evolving into a cavitation bubble. Such cavitation bubbles have long been studied, by a variety of techniques [21,27]. The high-speed photographic technique, pioneered by Lauterborn [27], is very helpful in visualizing the cavitation bubble's temporal behavior (see Fig. II-3). As time passes, the cavitation bubble grows in size, reaching a maximum dimension which can be related to the energy of the bubble. The bubble then collapses. At the time of collapse, another acoustic transient is emitted, of energy somewhat smaller than that in the shock/acoustic transient. The cycle of growth to a maximum followed by collapse and emission of an acoustic transient may repeat several times before the cavitation bubble finally dissipates. The energy in the cavitation bubble, determined from its first maximum, is found to reach 7.5% of the energy in the incident laser pulse [24]. It is worthwhile to note that the maximum cavitation bubble radius has been shown experimentally to scale as the 1/3 power of the incident laser energy [16], for a range of laser energies spanning nearly three orders of magnitude. This result provides an excellent confirmation of the classic relationship derived by Rayleigh [28].

Quantitative information on cavitation bubble pressure can be obtained from the combination of pump-probe time resolved measurements with hydrophone recordings of acoustic transients [24]. For a hydrophone located 10 mm away from the laser focus in 0.1N saline, pressures ranging from 50 bar for a 1.2 mm maximum diameter cavitation bubble up to 450 bar for a 5 mm maximum diameter cavitation bubble were obtained. The pressure scaled linearly with bubble maximum radius.

With quantitative information in hand on the energies going into the cavitation bubble and first acoustic transient, we can make order of magnitude comparisions with the phenomena shown in Fig. 1. Vaporization and ionization receive energy directly from the laser light while the acoustic transient and cavitation bubble receive their energy from the vaporization and ionization. Let us assume that the laser light is absorbed in a cylinder with radius 6.5 μm (see Ref. 24) and length 362 μm (see Eq. 5 in Ref. 20) for a 4 mJ laser pulse with breakdown threshold of 0.7 mJ. Let us further assume the plasma temperature of 15,000 deg. Kelvin (1.29 eV) as given in [17], the only spectroscopic temperature determination of which we are aware. Then the amounts of energy estimated to be needed for vaporization and ionization are 0.11 mJ and 0.60 mJ respectively. These energies, although rough estimates, are comparable to the energies found experimentally for the acoustic transient and the cavitation bubble, 0.14 mJ and 0.30 mJ respectively [24].

C. Effects of the Laser-Produced Plasmas

Laser produced plasmas in ophthalmology have a wide range of effects. These include such direct effects as mem-

brane destruction in the posterior capsulotomy and iridotomy and indirect effects such as plasma shielding of the retina and retinal damage by acoustic waves. Research both *in vivo* and *in vitro* has tried to determine the importance and risks of these direct and indirect effects and suitable laser parameters to accomplish the desired therapies while minimizing deleterious consequences.

Tissue disruption, the most striking effect of laser produced plasmas in ophthalmology, was investigated *in vitro* using three different model systems [25,29,30]. In order to separate the effect of the plasma from that of the acoustic transient and cavitation bubble, the authors chose illumination geometries both parallel to (focus located tens to hundreds μm above the surface) and perpendicular to the target surface. Beilin et al. used a single cellular layer of onion skin [29] (laser wavelength 1.06 μm, pulse lengths 30 ps or 10 ns, energy up to 8 mJ or 50 mJ); Vogel et al. studied a polyethylene membrane [25] (laser wavelength 1.06 μm, pulse lengths 30 ps or 7 ns, energy up to 5 mJ or 15 mJ); and Zysset et al. investigated corneal endothelium [30] (laser wavelength 1.06 μm, pulse lengths 40 ps or 10 ns, energy up to 25 mJ or 200 mJ). Perforation of the membranes was determined to occur only when the plasma was in contact with the membrane [25,29]. Acoustic transients and cavitation bubbles were not able to produce a membrane perforation. Zysset et al. [30] found however, that with the parallel focusing geometry, corneal endothelial cells could be damaged or removed and the underlying (Descemet's) membrane ruptured solely by acoustic transients and cavitation bubbles. The authors showed that the range of the damage scaled as the cube root of the laser energy [30]. The maximum radius of a cavitation bubble is known to scale in this same manner [16, 26]. Thus sensitive structures like corneal endothelium damage from acoustic transients and cavitation bubbles while perforation of more robust structures appear to require direct contact with the plasma.

Plasma shielding was investigated by Steinert et al. [12] , [13] and by Docchio et al. [31]. Once breakdown occurs and the plasma is formed, laser light which continues to fall upon the focal volume is absorbed, reflected or scattered. Thus the plasma shields structures within the eye (such as the retina) beyond the focal point. The straight-through energy transmission of a laser beam focused in saline was measured. It was found that once threshold is exceeded, the plasma substantially reduces energy transmission along the laser beam path. The measured energy reduction appears to lie in the range of 23% to 56% of the incident laser energy, for intensities above breakdown threshold. No systematic study of the energy reflected or scattered from the focal region was undertaken. The energy above that required to achieve breakdown likely is scattered, reflected and absorbed, providing additional local heating and pressure increase in the focal volume.

The ability to localize disruption within the eye to scales of a few μm improves as the laser pulse length is reduced. Zysset et al. have used time integrated luminescence to measure plasma dimensions of 30 μm length and 8 μm width for ps Nd:YAG laser pulses at 8 μJ [16]. Because the size of the damage zone scales as the cube root of the laser energy [30], lower energies are expected to produce more localized damage. Incisions in corneal tissue, using ps and fs pulses, show characteristically smooth walls and minimal subsurface damage for energies in the tens of μJ range for 532 and 625 nm lasers [32]. The incisions compare very well with those obtained using excimer lasers which rely on a photo-chemical rather than a plasma-mediated process for ablation. Surgery in the vitreous, very near the retina, may now be possible bt the use of these short pulse, low energy lasers.

III. LASER PRODUCED PLASMAS IN UROLOGY & GASTROENTEROLOGY

The laser was first proposed for use in urology to fragment kidney stones, more than two decades ago, and experiments with pulsed ruby and CW CO_2 lasers confirmed the utility of the approach [33]. Ten years later, Fair [34] showed that stones (also referred to as calculi) could be successfully fragmented by ruby laser (1.8 J energy, 20 ns pulse) induced stress waves with pressures above about 3.2 kbar. The ability to produce such stress wave pressures depended on the presence of a laser produced plasma at the surface of the stone. It was not until the decade of the 1980's that suitable fiber-optic delivery systems were devised [35 - 37] which made laser mediated lithotripsy (literally, stone breaking) a clinical reality [38 - 40]. Progress with laser lithotripsy of gallstones has followed closely the work on kidney stones [41] and clinical success has been achieved here as well [42]. It is worth noting that ultrasound lithotripsy, which dates from the mid 1970's, is probably the more popular of the non-surgical techniques available today for destroying and removing calculi. The laser mediated approach, however, offers advantages, possibly for elderly patients and for patients whose calculi are impacted or rest in areas where the ultrasound technique is ineffective.

In laser mediated lithotripsy, laser pulses from a high power dye laser (typical wavelength 0.5 - 0.7 μm, pulse-

length 1 μs, fluence of tens of J/cm^2, pulse repitition rate 5 Hz) are delivered to the stone via a fiber optic cable passed into the body endoscopically. The fiber optic tip is either in contact with or within a few mm of the stone. Tens to hundreds of laser pulses are needed to fragment stones of most material compositions. The small fragments which result are then passed out of the body spontaneously, by irrigation or removed by further procedures. Success rates in clinical studies in excess of 90% have been reported with little evidence of collateral damage [38 - 40]. *In vitro* experiments have shown that, in order for fragmentation of the kidney stones or gallstones to occur, a plasma must be present.

A. Phenomena for $0 \leq t \leq \tau_{laser}$

The physical phenomena present include laser absorption and plasma production at the stone surface followed by plasma growth. After the plasma is initiated, inverse bremsstrahlung is likely the mechanism for further absorption of the laser light within the plasma, which now shields the solid surface. After the peak of the laser pulse, the plasma decays, on roughly the same time scale as the laser pulse. In an experiment in which gallstones were irradiated by flash-lamp pumped dye lasers (0.4-0.7 μm wavelength, 0.8 or 360 μs pulse length, 1.5 or 0.1 J maximum energy), measurements were made of time resolved, broad-band (.35 to .45 μm wavelengths) emission from the laser produced plasma [43]. The laser energy was transported to the stone via a 300 μm core diameter fiber optic cable. Information on the time of plasma initiation and the duration of the plasma luminescence was obtained. The experiments showed that a certain time elapses between the beginning of the laser pulse and the onset of visible light emission [cf. Refs. 15 & 31]. The energy deposited during this time, referred to as the threshold energy, is found to be roughly independent of laser pulse width. Threshold fluences for the 0.8 μs pulses ranged from 4 to 12 J/cm^2, corresponding to energies of 2.8 to 8.5 mJ. It was found that once the plasma initiation occurred and the peak emission had been achieved, the luminescence decayed with a slightly longer time scale than the driving laser pulse.

Using a gated optical multichannel analyzer and a spectrograph (resolution 0.5 nm), measurements were also made of time-resolved visible emission spectra [43]. The spectra show a broad continuum with line spectra from neutral and singly ionized Ca superimposed. For a time well after the end of the laser pulse, the continuum disappears leaving a rich line spectrum. Analysis of the spectra yields electron density of the plasma in the 10^{19}/cm^3 range [43,44] consistent with modeling using a one dimensional hydrocode [45]. Estimates of the electron temperature were obtained as well. Spectral analysis yielded a temperature of about 15,000 deg. K. [44] while hydrocode modeling gave a temperature of about 5,000 deg. K. [45]. Further experimental work and modeling will be needed to resolve this disagreement.

B. Phenomena for $t > \tau_{laser}$

After the laser pulse ends, the plasma expands rapidly and cools. High pressure stress/acoustic waves are generated which propagate into the stone and the surrounding medium. In an experiment using gallstones and kidney stones immersed in water, measurements were made of the stress waves propagating through the stones, and the acoustic waves and cavitation bubble which were found in the liquid [46]. The stress waves were measured using an optoacoustic technique (deflection of a probe He-Ne laser beam by an index of refraction change induced by stress wave propagating in a fixture supporting the stone) and a piezoelectric technique (stone is resting directly on a piezoelectric element). These two measurements agreed and showed that a tenfold increase in signal strength was achieved by immersing the stone in at least .3 cm of water. A similar increase (4 to 5 times) was noted in modeling the plasma pressure directly, for stones in water compared with stones in air [45]. The increased pressures certainly responsible for causing the observed signals are due to the confinement of the plasma between the solid stone and the water [47]. It was also found that the stress wave signal strength scaled as the 1/2 power of the laser fluence, consistent with an ideal gas model [48].

The acoustic transient was measured by a pump-probe laser technique [cf. Ref. 14]. The acoustic transient propagated at the local sound speed, with no evidence of the hypersonic speeds measured by others [14,16]. Time resolved measurements were also made of the evolution of the cavitation bubble, using the pump-probe laser technique and microsecond duration flash photography [46,49]. The cavitation bubble grows, reaches a maximum size and collapses. With maximum measured radii r_{max} of 0.3 cm and 0.42 cm for laser fluences of 21 and 90 J/cm^2 respectively, r_{max} propor-

tional to the 1/3 power of laser pulse energy is satisfied [28] as we have seen above [cf. Ref. 16]. Using the fact that a photograph taken at time 3.6 μs (relative to the beginning of the laser pulse at t=0) shows the fiber optic tip to have been displaced, one can estimate that a 1 kbar pressure was required to achieve the observed displacement [46,49]. This pressure is consistent with other experiments [24,34] and with model studies [45].

C. Effects of the Laser-Produced Plasmas

The motivation for the gallstone and kidney stone research cited above is that pulsed medical lasers can fragment most types of stones with relative ease. Several studies have been done to quantify the fragmentation effects of dye lasers [50 - 52]. Fragmentation threshold, defined as the minimum energy required to produce visible damage on the surface of a target stone, was measured for kidney stones [51,52] and gallstones [50,52]. Gallstones showed a uniformly lower fragmentation threshold than all types of kidney stones. Bhatta & Nishioka report a threshold of 3.9 mJ for gallstones and a range of 4.5 to 41 mJ for fragmentable kidney stones (504 nm laser wavelength, 1 μs pulse length, 200 μm diameter optical fiber) [52]. Longer pulse lengths (8 microsec) give slightly higher thresholds [see Table 1, Ref. 52]. Watson et al. showed that for kidney stones threshold increases with wavelength and fiber diameter [see Tables 1 and 3, Ref. 51].

Fragmentation rate, defined as the amount of mass removed from a stone per laser pulse, has also been investigated for gallstones and kidney stones [50 - 52]. In general, it was found that for stones immersed in water or saline, the higher laser pulse energies yielded higher fragmentation rates and larger stone fragments. Fragmentation rates decrease with increasing laser pulse length. Bhatta and Nishioka have found a fragmentation rate of 1.1 mg/pulse for a struvite urinary calculus (50 mJ pulse energy, 504 nm laser wavelength, 1 μs pulse length, 200 μm diameter optical fiber) [52]. At the same laser wavelength and pulse energy, Watson et al. found a rate of .035 mg/pulse for a calcium oxalate calculus (1.5 μs pulse length, 600 μm diameter optical fiber) [51]. This difference in fragmentation rate may be due to the higher fluence used or to important variations in kidney stone material properties.

D. Proposed Mechanism

The mechanism proposed [53] to explain the laser-calculus interaction proceeds as follows. The laser interacts with the opaque stone surface producing a thin localized heated layer. As the heating continues, there is vaporization, liberation of free electrons and plasma formation. Alternatively, there can be material desorption from the stone surface followed by heating and free electron creation in the desorbed material [54]. The plasma continues to absorb the laser light, likely by inverse bremsstrahlung absorption. Then the plasma expands either freely (in air) or mechanically constrained (in water) and creates a back pressure on the stone surface. Evidence of this back pressure has been seen experimentally in the rapid recoil of the fiber optic delivery cable on time scales of the order of a few μs [46]. The pressure induces strong acoustic waves (stress waves) within the stone material [46]. These waves are compressive stress waves initially. Upon reflection from internal stone inhomogeneities or from the stone-air or stone-water interface, the waves become tensile stress waves of sufficient strength to fragment the stone [55]. Alternatively, a fragmentation shock wave may propagate through the porous stone material, most efficiently removing material when the laser pulse energy just exceeds the fragmentation threshold [44].

IV. LASER PRODUCED PLASMAS IN CARDIOLOGY & VASCULAR SURGERY

Because coronary heart disease is one of the leading causes of mortality in the developed world, the prospect of using lasers to clear plaque filled arteries is very exciting. The procedure, known as laser angioplasty, has been in clinical use for several years. Laser angioplasty utilizes fiberoptic delivery of CW laser radiation to the coronary or peripheral arteries and proceeds by either heating a metal probe which melts the plaque or by direct illumination and ablation of the plaque. CW lasers work well with soft plaque deposits but have not been able to ablate heavily calcified plaque. The process is not without its problems. These include arterial wall perforation, aneurysms, pain and spasm which result from injury of normal tissue adjacent to or underlying the plaque.

Laser produced plasmas in this area of medicine have not yet reached the clinical setting. Several studies [56 - 60] have shown that the phenomena which we have discussed above, namely visible light emission, acoustic transients and material removal, are all present here. Laser pulses of short duration (tens of ns to tens of μs), moderate energy (tens to 100 mJ), and small spot diameters (hundreds of μm to a few mm) with wavelengths from 193 nm to 658 nm were

used. Studies were all done *in vitro* for atherosclerotic and normal arterial samples in air, saline or blood. We discuss below the phenomena and the effects.

A. Phenomena for $0 \leq t \leq \tau_{laser}$

During the laser pulse, a plasma is formed which emits light at visible wavelengths. The plasma likely persists for the duration of the laser pulse (although no measurements of this plasma's lifetime have been reported). Experiments were performed with excimer [59] and dye [57] lasers to obtain time integrated [59] or time-resolved [57] emission spectra, and time-integrated plasma luminescence [57] (see Fig. IV-1). In the work of Clarke et al. [59], pulsed excimer lasers (wavelengths 193 nm, 248 nm, 308 nm and 351 nm; energy 100 to 250 mJ; spot dimensions 1 x 5 mm) were used to irradiate carviovascular tissues exhibiting atherosclerosis. Plasma formation was always observed for tissue samples in air but never for experiments in water (although the authors showed plasma production in water with a highly absorbing graphite target). Time-integrated visible light spectra showed the rich line structure similar to those observed in the case of laser irradiation of gallstones [43]. Prince and co-workers [57] used a dye laser (wavelength 658 nm, energy approximately 100 mJ, pulse length 0.8 μs) to irradiate both calcified arterial plaque and normal artery. They found an emission spectrum, taken during the laser pulse, which exhibited line structure and a superimposed continuum [c.f. Ref. 43] (see Fig. IV-2). The presence of ionized Ca lines confirmed that a plasma was present. A time-integrated photograph of the luminescence (see Fig. IV-1) provides graphic evidence for the presence of plasma for laser irradiation of calcified arterial plaque.

A crucial problem for CW laser angioplasty and plasma-mediated laser angioplasty is how to know whether the laser is encountering arterial plaque or healthy tissue. The unique presence of Ca lines in emission spectra, detected in light which returns through the same fiber used for irradiation, offers the prospect of an unequivocal diagnostic [59]. Broadband light emission was also observed by Bhatta, Rosen and Dretler [60] who used it and the concomitant acoustic emission as a tandem diagnostic to discriminate calcified plaque from normal artery.

B. Phenomena for $t > \tau_{laser}$

Following the laser pulse, acoustic wave emission takes place. Observations of a loud snapping sound accompanying plasma production were reported in all the cited references [56 - 60]. Acoustic signals were detected by a hydrophone (with frequency response to 350 kHz), in the experimental work of Bhatta, Rosen & Dretler [60] . A dye laser (wavelength 504 nm, energy 5-50 mJ, pulse duration 1.4 μs) was used to irradiate specimens of human aorta with calcified plaque, soft plaque, and normal arterial wall. The acoustic signals, occurring along with plasma light emission signals, provided a unique signature for laser ablation of calcified or soft arterial plaque in blood. Normal arterial wall produced negligible acoustic and plasma light emission signals while blood alone yielded strong acoustic signals only. The structure seen at early time in the hydrophone signals may be due to the initial acoustic transient and first few collapses of a cavitation bubble [c.f. Refs. 24 & 25].

C. Effects of the Laser-Produced Plasmas

The object of laser angioplasty is to efficiently remove atherosclerotic plaque with minimal effect to underlying healthy tissue and minimal collateral impact on the vascular system. To accomplish this task, optimum laser parameters of wavelength, pulse length and pulse energy need to be identified. *In vitro* studies [56 - 58] have begun this process; ablation thresholds, ablation rates and characteristics of ablation fragments have been investigated. The ablation threshold is the laser energy at which observable tissue ablation is obtained. The ablation rate (or ablation efficiency) is the mass removed divided by the total energy delivered.

Ablation thresholds were measured for several laser wavelengths, in saline and air, for calcified plaque and normal artery [57]. General conclusions are that the dye laser (wavelengths 450 to 700 nm, pulse duration 1 μs) yields thresholds for calcified plaque lower by more than a factor of two than the ablation thresholds for normal artery. For example, at 482 nm wavelength, the threshold for calcified plaque in air or water is 34 mJ compared to the 80 mJ threshold for normal artery. The effect of laser pulse length on ablation threshold was studied by LaMuraglia et al. [58] at 480 nm. Thresholds generally increased with increasing pulse length reaching 90 mJ for calcified plaque and 131 to 169 mJ for three types of normal arterial wall tissue at 50 μs pulse length.

Systematic measurements of ablation rates were made [56 - 58] for normal artery and calcified and fibrous plaque using a dye laser (wavelength 480 nm). In general, every sample of atherosclerotic plaque ablated more efficiently than every sample of normal artery. Ablation in saline was more efficient than ablation in air. Finally, efficiency showed a marked drop for a 50 μs laser pulse compared to results at 1 and 8 μs. The important lesson to be learned from the data [see Table 1 of Ref. 56, Table 2 of Ref. 57, and Table II of Ref. 58] is that the plasma-mediated ablation process for dye lasers is very selective. That is, it is considerably easier to ablate calcified or fibrous plaque than it is to ablate normal artery for the same laser conditions. For example, the ablation rate for calcified plaque is 4.1 mg/J while normal artery ablates at a rate of .05 mg/J for 80 mJ pulses, 1 μs in duration [58] (see Fig. IV-3 for a compilation of ablation rates).

Laser angioplasty removes undesirable material from the arteries. If the plasma-mediated approach is to be adopted clinically, detailed knowledge of the sizes of removed particulate material must be known. Such material may be large enough to block small arteries, if the particulates enter the blood stream. The ablation of calcified plaque by dye laser under saline produces debris [56,57]. Microscopic examination shows that tissue fragments and occasional cholesterol crystals are present [56,57]. Most of the fragments are under 20 μm in size although there are occasional fragments up to 100 μm. No systematic examination of these fragments has been made, however.

V. CONCLUSION

Much has been learned, over the last 25 years, of laser-produced plasmas in medicine with regard to the plasma phenomena present and the plasma's direct and indirect effects. We expect that future work in ophthalmology will take advantage of the localizability possible with the shorter laser pulse lengths and lower threshold energies. Laser lithotripsy will continue to provide an alternative therapy choice to ultrasound lithotripsy. We look for the introduction of percutaneous (through the skin) procedures in the area of gallstone lithotripsy. New avenues are anticipated in plasma-mediated laser angioplasty, particularly ones which take advantage of the efficiency of material removal of the calcified plaque and solve the problem of release of particulates into the blood. Progress in all these areas must rely upon further *in vitro* research on plasma and mechanical tissue characterization and theoretical modeling.

REFERENCES

*Work performed under the auspices of the United States Department of Energy.

1. D.E. Thomsen, "Plasma Physics Breaks Stones," Science News **130**, 157 (1986).
2. J.-L. Boulnois, "Photophysical Processes in Recent Medical Laser Developments: A Review," Lasers in Medical Science **1**, 47 (1986).
3. M.M. Krasnov, "Q-Switched Laser Goniopuncture," Arch. Ophthalmol **92**, 37 (1974).
4. M.S. Bass, C.V. Cleary, E.S. Perkins & C.B. Wheeler, "Single Treatment Laser Iridotomy," Brit. J. Ophthalmol **92**, 29 (1979).
5. E. van der Zypen, H. Bebie & F. Fankhauser, "Morphological Studies about the Efficiency of Laser Beams upon the Structures of the Angle of the Anterior Chamber - Facts and Concepts Relating to the Treament of Chronic Simple Glaucoma," Int. Ophthal. **1**, 109 (1979).
6. D. Aron-Rosa, J.J. Aron, M. Griesemann & R. Thyzel, "Use of the Neodymium YAG Laser to Open the Posterior Capsule After Lens Implant Surgery. A Preliminary Report," J. Am. Intraoc. Implant Soc. **6**, 352 (1980)
7. A.L. Robin & I.P. Pollack, "The Q-Switched Ruby Laser in Glaucoma," Ophthalmology **91**, 366 (1984).
8. S. Lerman, B. Thrasher & M. Moran, "Vitreous Changes after Nd:YAG Laser Irradiation of the Posterior Lens Capsule or Mid-Vitreous," Am. J. Ophthalmol. **97**, 470 (1984).
9. M. L. Wolbarsht, "Ophthalmic Uses of Lasers," in **Lasers in Biology & Medicine**, F. Hillenkamp, R. Pratesi & C. A. Sacchi, eds. (Plenum, New York, 1980).
10. M.A. Mainster, D.H. Sliney, C.D. Belcher & S.M. Buzney, "Laser Photodisruptors - Damage Mechanisms, Instrument Design & Safety," Ophthalmol. **90**, 973 (1983).
11. J.F. Ready, **Effects of High-Power Laser Radiation**, (Academic, New York, 1971), p.187-191.
12. R.F. Steinert, C.A. Puliafito & C. Kittrell, "Plasma Shielding by Q-Switched & Mode-Locked Nd:YAG Lasers," Ophthalmology **90**, 1003 (1983).
13. R.F. Steinert, C.A. Puliafito & S. Trokel, "Plasma Formation & Shielding by Three Ophthalmic Nd:YAG La-

sers," Am. J. Ophthalmol. 96, 427 (1983).
14. J.G. Fujimoto, W.Z. Lin, E.P. Ippen, C. A. Puliafito & R.F. Steinert, "Time-Resolved Studies of Nd:YAG Laser-Induced Breakdown," Invest. Ophthalmol. Vis. Sci. 26, 1771 (1985).
15. F. Docchio, L. Dossi & C.A. Sacchi, "Q-Switched Nd:YAG Laser Irradiation of the Eye & Related Phenomena: An Experimental Study. I. Optical Breakdown Determination for Liquids & Membranes," Lasers Life Sci. 1, 87 (1986).
16. B. Zysset, J. G. Fujimoto & T. F. Deutsch, "Time-Resolved Measurements of Picosecond Optical Breakdown," Appl. Phys. B 48, 139 (1989).
17. P.A. Barnes & K.E. Rieckhoff, "Laser Induced Underwater Sparks," Appl. Phys. Lett. 13, 282 (1968).
18. F. Docchio, P. Regondi, M.R.C. Capon & J. Mellerio, "Study of the Temporal & Spatial Dynamics of Plasmas Induced in Liquids by Nanosecond Nd:YAG Laser Pulses. 2: Plasma Luminescence & Shielding," Appl. Opt. 27, 3669 (1988).
19. F. Docchio, "Lifetimes of Plasmas Induced in Liquids & Ocular Media by Single Nd:YAG Laser Pulses of Different Duration," Europhys. Lett. 6, 407 (1988).
20. F. Docchio, P. Regondi, M.R.C. Capon & J. Mellerio, "Study of the Temporal & Spatial Dynamics of Plasmas Induced in Liquids by Nanosecond Nd:YAG Laser Pulses. 1: Analysis of the Plasma Starting Times," Appl. Opt. 27, 3661 (1988).
21. M.P. Felix & A.T. Ellis, "Laser-Induced Liquid Breakdown - a Step-By-Step Account," Appl. Phys. Lett. 19, 484 (1971).
22. E. F. Carome, C. E. Moeller & N. A. Clark, "Intense Ruby Laser-Induced Acoustic Impulses in Liquids," J. Acoust. Soc. Am. 40, 1462 (1966).
23. C. E. Bell & J. A. Landt, "Laser-Induced High Pressure Shock Waves in Water," Appl. Phys. Lett. 10, 46 (1967).
24. A. Vogel & W. Lauterborn, "Acoustic Transient Generation by Laser Produced Cavitation Bubbles Near Solid Boundaries," J. Acoust. Soc. Am. 84, 719 (1988).
25. A. Vogel, W. Hentschel, J. Holzfuss & W. Lauterborn, "Cavitation Bubble Dynamics and Acoustic Transient Generation in Ocular Surgery with Pulsed Neodymium:YAG Lasers," Ophthalmology 93, 1259 (1986).
26. R. H. Cole, Underwater Explosions, (Princeton University Press, Princeton, NJ. 1948).
27. W. Lauterborn, "High-Speed Photography of Laser-Induced Breakdown in Liquids," Appl. Phys. Lett. 21, 27 (1972).
28. J. W. Rayleigh, "On the Pressure Developed in a Liquid During the Collapse of a Spherical Cavity," Phil. Mag. 34, 94 (1917).
29. E. N. Beilin, A. Yu. Bayanov-Uzdal'skii, V. P. Zharov, V. I. Loshchilov, G. V. Mishakov & S. V. Chekalin, " Laser-Acoustical Phenomena in Water and Their Influence on Cell Structures," Sov. Phys. Acoust. 33, 119 (1987).
30. B. Zysset, J. G. Fugimoto, C. A. Puliafito, R. Birngruber & T. F. Deutsch, "Picosecond Optical Breakdown: Tissue Effects and Reduction of Collateral Damage," Lasers Surg. Med. 9, 193 (1989).
31. F. Docchio, L. Dossi & C.A. Sacchi, "Q-Switched Nd:YAG Laser Irradiation of the Eye & Related Phenomena: An Experimental Study. II. Shielding Properties of Laser-Induced Plasmas in Liquids & Membranes," Lasers Life Sci. 1, 105 (1986).
32. D. Stern, R. W. Schoenlein, C. A. Puliafito, E. T. Dobi , R. Birngruber & J. G. Fugimoto, "Corneal Ablation by Nanosecond, Picosecond & Femtosecond Lasers at 532 and 625 nm," Arch. Ophthalmol 107, 587 (1989).
33. W. P. Mulvaney & C. W. Beck, "The Laser Beam in Urology," J. Urol. 99, 112 (1968).
34. H. D. Fair, "In Vitro Destruction of Urinary Calculi by Laser-Induced Stress Waves," Med. Instrum. 12, 100 (1978).
35. J. Pensel, F. Frank, K. Rothenberger, A. Hofstetter & E. Unsold, "Destruction of Urinary Calculi by Nd:YAG Laser Radiation," in Laser Surgery IV. Proceedings of Fourth International Symposium on Laser Surgery, ed. Kaplan. Chapter 10, pps 4 - 6. Jerusalem: Academic Press.
36. G. M. Watson, J. E. A. Wickham, T. N. Mills, S. G. Bown, P. Swain & P. R. Salmon, "Laser Fragmentation of Renal Calculi," Brit. J. Urol. 55, 613 (1983).
37. G. M. Watson, S. L Jacques, S. P. Dretler, and J. A. Parrish, "Tunable Pulsed Dye Laser for Fragmentation of Urinary Calculi," Lasers Surg. Med. 5, 160 (1985) (Abstract).
38. S. P. Dretler, G. M. Watson, S. Murray and J. A. Parrish, "Laser Fragmentation of Ureteral Calculi: Clinical Experience," Lasers Surg. Med. 6, 191 (1986) (Abstract).

GITOMER

39. G. M. Watson & J. E. A. Wickham, "Initial Experience with a Pulsed Dye Laser for Ureteric Calculi," Lancet **8494**, 1357, Jun. 14, 1986.
40. S. P. Dretler, G. Watson, J. A. Parrish & S. Murray, "Pulsed Dye Laser Fragmentation of Ureteral Calculi: Initial Clinical Experience," J. Urol. **137**, 386 (1987).
41. N. S. Nishioka & R. R. Anderson, "Fragmentation of Biliary Calculi with Tunable Dye Lasers," Gastrointest. Endosc. **32**, 157 (1986) (Abstract).
42. G. Lux, Ch. Ell, J. Hochberger, D. Muller, L. Demling, " The First Endoscopic Retrograde Laser Lithotripsy of Common Bile Duct Stones in Man Using a Pulsed Neodymium YAG Laser," Endoscopy **18**, 144 (1986).
43. P. Teng, N. S. Nishioka, R. R. Anderson, and T. F. Deutsch, "Optical Studies of Pulsed-Laser Fragmentation of Biliary Calculi," Appl. Phys. B **42**, 73 (1987).
44. D. Rosen, G. Weyl, G. Simons, H. Petschek & L. Popper, "Modeling of the Laser-Induced Thermal Response, Ablation, and Fragmentation of Biological Tissue," Report PSI TR-765, April 1988, Physical Sciences, Inc., Research Park, P.O. Box 3100, Andover, MA 01810 (unpublished).
45. S.J. Citomer, R.D. Jones & C. Howsare, "Modeling of Laser Ablation & Fragmentation of Human Calculi," SPIE Vol. 1066, Laser Surgery: Advanced Characterization, Therapeutics, and Systems (1989), p. 145.
46. P. Teng, N. S. Nishioka, R. R. Anderson, and T. F. Deutsch, "Acoustic Studies of the Role of Immersion in Plasma-Mediated Laser Ablation," IEEE J. Quant. Electron. **QE-23**, 1845 (1987).
47. N. C. Anderholm, "Laser-Generated Stress Waves," Appl. Phys. Lett. **16**, 113 (1970).
48. A. J. Campillo, R. D. Griffin & P. E. Schoen, "Reflective Probing of Laser Generated Multi-kbar Compressional Shocks in Water," Opt. Commun. **57**, 301 (1986) and R. D. Griffin, B. L. Justus, A. J. Campillo & L. S. Goldberg, "Interferometric Studies of the Pressure of a Confined Plasma," J. Appl. Phys. **59**, 1968 (1986).
49. P. Teng, N. S. Nishioka, W. A. Farinelli, R. R. Anderson & T. F. Deutsch, "Microsecond-Long Flash Photography of Laser-Induced Ablation of Biliary & Urinary Calculi," Lasers Surg. Med. **7**, 394 (1987).
50. N.S. Nishioka, Paul C. Levins, S.C. Murray, J.A. Parrish, and R.R. Anderson, "Fragmentation of Biliary Calculi with Tunable Dye Lasers," Gastroent. **93**, 250 (1987).
51. G. M. Watson, S. Murray, S. P. Dretler & J. A. Parrish, "The Pulsed Dye Laser for Fragmenting Urinary Calculi," J. Urol. **138**, 195 (1987).
52. K. M. Bhatta & N. S. Nishioka, "Effect of Pulse Duration on Microsecond-Domain Laser Lithotripsy," Lasers Surg. Med. **9**, 454 (1989).
53. N. S. Nishioka, P. Teng, T. F. Deutsch, and R. R. Anderson, "Mechanism of Laser-Induced Fragmentation of Urinary and Biliary Calculi," Lasers in the Life Sciences **1**, 231 (1987).
54. S. E. Egorov, V. S. Letokhov, and A. N. Shibanov, "Mechanism for Ion Formation by Irradiation of Molecular Crystal Surfaces with Laser Pulses," Sov. J. Quantum Electron. **14**, 940 (1984).
55. H. Kolsky, Stress Waves in Solids, (Dover, New York, 1963).
56. M. R. Prince, T. F. Deutsch, A. H. Shapiro, R. J. Margolis, A. R. Oseroff, J. T. Fallon, J. A. Parrish & R. R. Anderson, "Selective Ablation of Atheroma Using Flashlamp-Excited Dye Laser at 465 nm," Proc. Natl. Acad. Sci. USA **83**, 7064 (1986).
57. M. R. Prince, G. M. LaMuraglia, P. Teng, T. F. Deutsch & R. R. Anderson, "Preferential Ablation of Calcified Arterial Plaque with Laser-Induced Plasmas," IEEE J. Quant. Electron. **QE-23**, 1783 (1987).
58. G. M. LaMuraglia, S. Murray, R. R. Anderson & M. R. Prince, "Effect of Pulse Duration on Selective Ablation of Atherosclerotic Plaque by 480- to 490-nanometer Laser Radiation," Lasers Surg. Med. **8**, 18 (1988).
59. R. H. Clarke, J. M. Isner, T. Gauthier, K. Nakagawa, F. Cerio, E. Hanlon, E. Gaffney, E. Rouse & S. DeJesus, " Spectroscopic Characterization of Cardiovascular Tissue," Lasers Surg. Med. **8**, 45 (1988).
60. K. Bhatta, D. I. Rosen & S. P. Dretler, "Acoustic & Plasma-Guided Laser Angioplasty," Lasers Surg. Med **9**, 117 (1989).
61. G. M. Watson, S. P. Dretler & J. A. Parrish, "The Pulsed Dye Laser for Fragmentation of Urinary Calculi," preprint, 1987 (unpublished).
62. J. T. Walsh & T. F. Deutsch, "Pulsed CO_2 Laser Tissue Ablation: Measurement of the Ablation Rate," Lasers Surg. Med. **8**, 264 (1988).
63. "Gall-Stone Lithotripsy," advertising literature for EMG 602 long pulse excimer laser, Lambdaphysik, Gottingen, West Germany, 1987 (unpubiished).

CITOMER

64. W. S. Grundfest, F. Litvack, J. S. Forrester, T. Goldenberg, H. J. C. Swan, L. Morgenstern, M. Fishbein, I. S. McDermid, D. Rider, T. J. Pacala & J. B. Laudenslager, "Laser Ablation of Human Atherosclerotic Plaque Without Adjacent Tissue Injury," J. Am. Coll. Cardiol. 5, 929 (1985).

TABLE 1. Optical breakdown threshold in physiological saline for Q-switched and mode-locked Nd:YAG lasers.

Reference	Wave Length (μm)	Pulse Length τ_{laser}	Spot Diam (μm)	Breakdown Threshold in Saline Energy (mJ)/pulse	Fluence (J/cm^2)	Intensity (W/cm^2)
Q-switched Nd:YAG laser:						
[10]	1.064	22 ns	50	6.8	347	1.6×10^{10}
[12]	1.064	15 ns	--	4.5	---	---
[13]	1.064	15 ns	--	.37,.78	---	---
[15]	1.064	7 ns	350	29.9	31.1	4.5×10^{9}
[15]	1.064	7 ns	230	18.9	45.5	6.5×10^{9}
[15]	1.064	7 ns	94	7.0	100.8	1.4×10^{10}
[15]	1.064	7 ns	50	3.4	175	2.5×10^{10}
[16]	1.06	10 ns	4	.38	3024	3.0×10^{11}
Q-switched Nd:YAG laser:						
[12]	0.532	15 ns	--	0.4	---	---
[14]	0.532	10 ns	--	6	---	---
Mode-locked Nd:YAG laser:						
[10]	1.064	30 ps	50	0.044	2.27	7.6×10^{10}
[12]	1.064	25 ps	--	0.04	---	---
[16]	1.06	40 ps	4	0.005	39.8	1.0×10^{12}

TABLE 2. Laser produced plasma lifetimes in liquids. I/I_{th} is the ratio of the experimental laser intensity to breakdown threshold intensity.

Laser	Wave Length	Pulse Length τ_{laser}	I/I_{th}	Plasma lifetime (FWHM)	Remarks, [Reference]
Nd:YAG	.532 μm	10 ns	3	10 ns	saline [14]
Ruby	.6943 μm	30 ns	—	30 ns	filtered, doubly distilled water [17]
Nd:YAG	1.064 μm	12 ns	5	3 - 12 ns	doubly distilled water, spatially dependent [18]
Nd:YAG	1.064 μm	12 ns	1	5.5 ns	distilled water [19]
Nd:YAG	1.064 μm	220 ps	1	400 ps	distilled water [19]
Nd:YAG	1.06 μm	40 ps	12	500 ps*	distilled water [16] *instrumental limit
Nd:YAG	1.06 μm	40 ps	250	1.5 ns	distilled water [16]
Nd:YAG	1.064 μm	30 ps	1	250 ps	distilled water [19]

Melting → **Vaporization** → **Bond Breaking** → **Ionization**

$334\ \rho(P_1,T_1)\ J/cm^3$ $2258\ \rho(P_2,T_2)\ J/cm^3$ $27{,}700\ \rho(P_3,T_3)\ J/cm^3$ $9632\ \varepsilon\ J/cm^3$

Fig. 1-1. Schematic display of physical processes with associated energy densities for increasing laser energy deposition on materials. ρ is the mass density (gm/cm^3) at pressure P_n and temperature T_n. ε denotes the energy in eV to which the material is being raised.

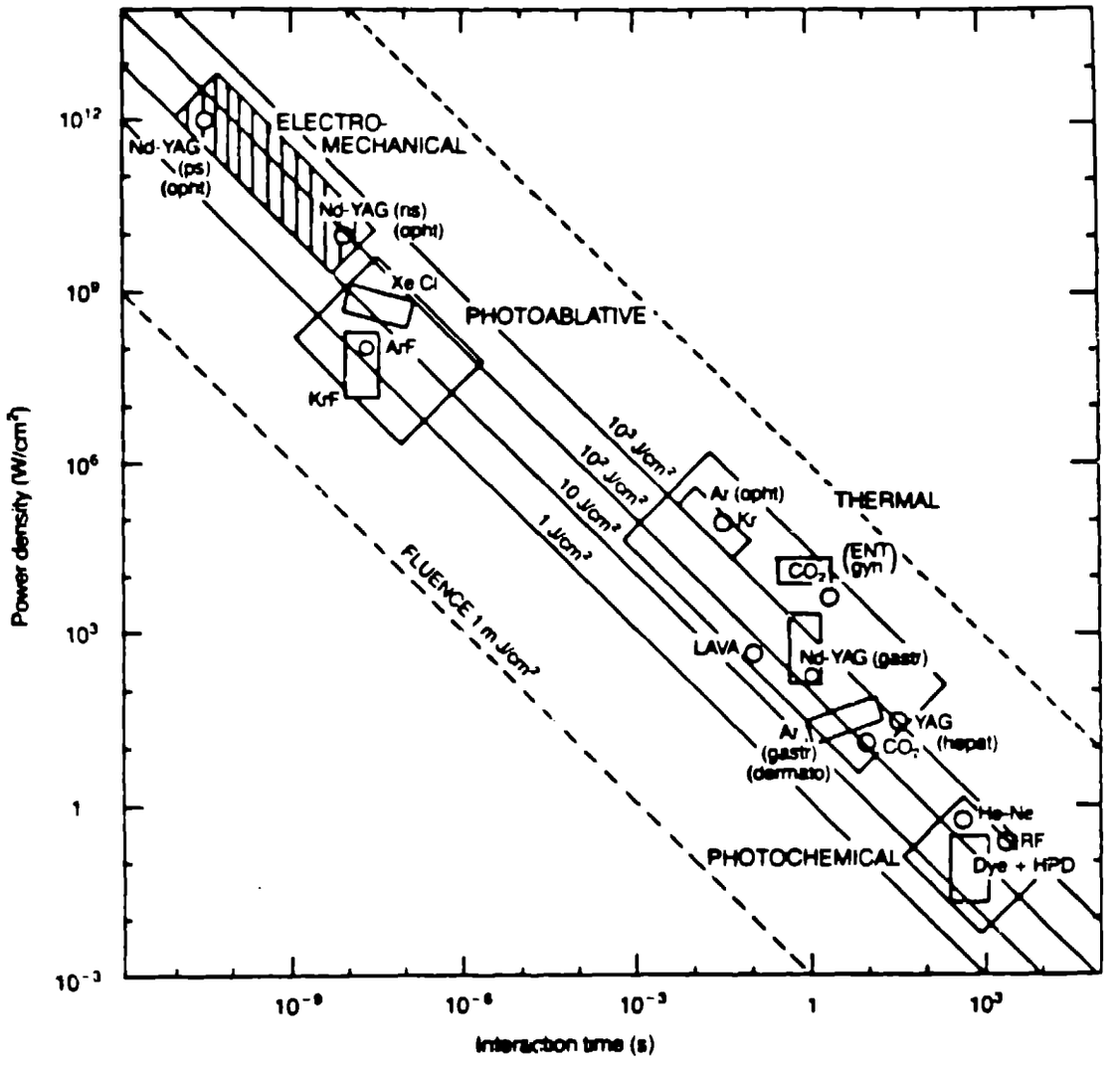

Fig. I-2 Medical laser interaction map. The ordinate shows the irradiance (in W/cm^2, on a logarithmic scale), and is commonly labelled the power density. The abscissa shows the interaction time. The diagonals show several lines of constant fluence (in J/cm^2). The boxed areas, labelled electromechanical, photoablative, thermal and photomechanical enclose points that correspond to more than 50 experimentally determined optimal values obtained from most published reports of clinical and experimental applications of lasers in medicine. Nd-YAG, neodymium-doped yttrium aluminum garnet laser; XeCL, xenon chloride laser; ArF, argon fluoride laser; KrF, krypton fluoride laser; Ar, argon laser; Kr, krypton laser; CO_2, carbon dioxide laser; LAVA, laser assisted vascular anastomosis; He-Ne, helium-neon laser; HPD, hematoporphyrin derivative; RF, radio frequency; ps, picosecond; ns, nanosecond; opth, ophthalmology; ENT, otorhinolaryngology; gyn, gynecology; gastr, gastrology; dermato, dermatology; hepat, hepatology. (Figure and caption from Ref. 2).

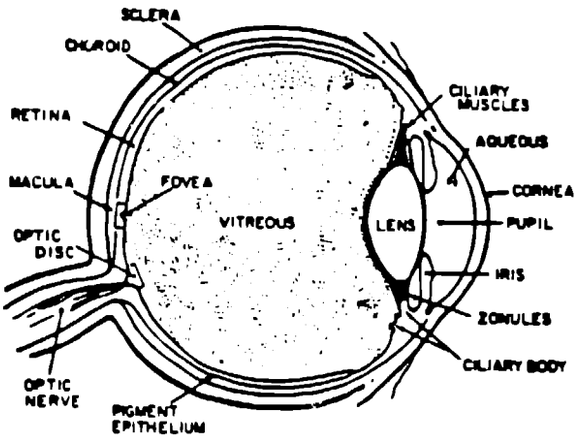

Fig. II-1. Schematic diagram of the human eye (Figure from Ref. 9).

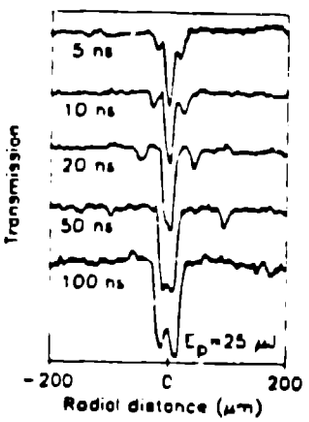

Fig. II-2. Spatial scans of probe laser transmission through plasma region between times 5 ns and 100 ns following 25 μJ, 40 ps Nd:YAG laser pulse. Horizontal axis measures distance from the laser focal point in water. Central feature evolves into a cavitation bubble; symmetric small features straddling the central feature show the shock wave (Figure from Ref. 16).

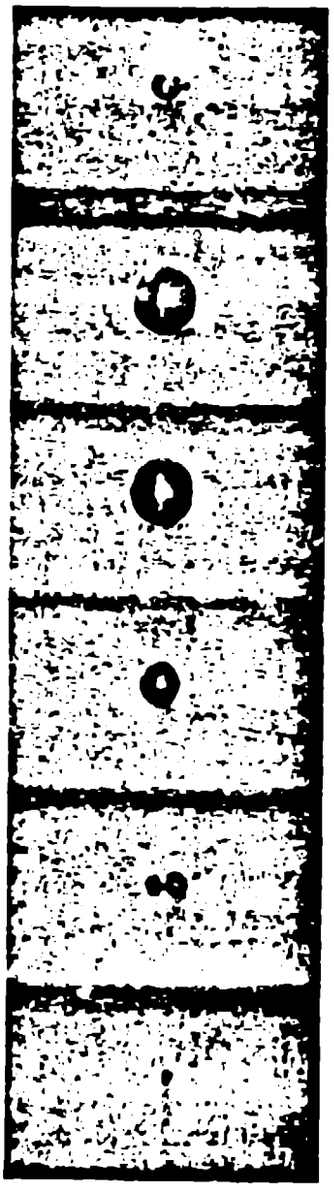

Fig. II-3. Optical breakdown and cavitation bubble evolution caused by focusing a 5mJ, 7 ns Nd:YAG laser pulse in saline. The bubble is back illuminated and the framing rate is 20,000 frames per second. Scale of black bar in final frame is 5 mm (Figure from Ref. 25).

Fig. IV-1. Luminescent ablation plume (plasma) from irradiation of calcified human arterial plaque with a single 100 mJ, 1 μs, 450 nm dye laser pulse. Scale is in mm (Figure from Ref. 57).

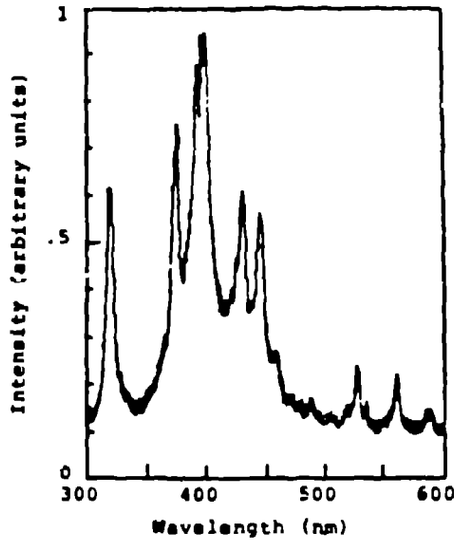

Fig. IV-2. Laser-induced emission spectrum from calcified human arterial plaque 0.6 μs after start of a 0.8 μs, 690 nm laser pulse. Continuum and ionized and neutral Ca emission lines are evident (Figure from Ref. 57).

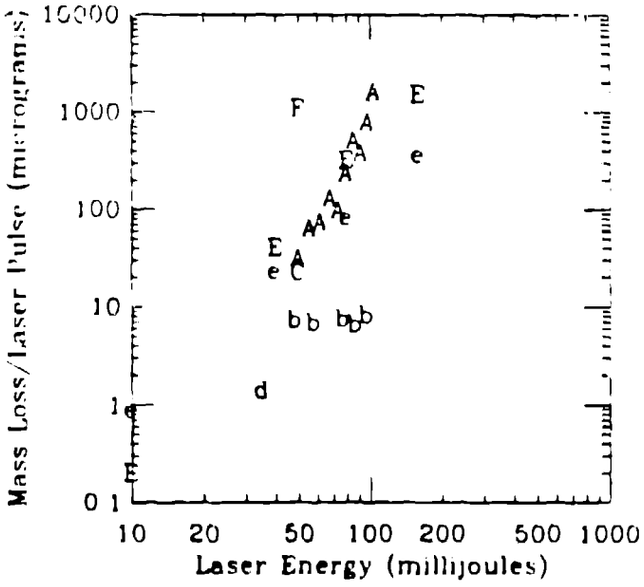

Fig. IV-3 Compilation of data on mass ablation efficiency. Mass loss per laser pulse (μg) is plotted versus laser pulse energy (mJ). Plasma production occurs in all cases. Hard tissue appears to be much easier to ablate than soft tissue. Legend: upper case letters for measurements in water, lower case letters for experiments in air; A - kidney stones, dye laser [61]; b - guinea pig skin; CO_2 laser [62]; C - gallstone, XeCl laser [63]; d - atherosclerotic aorta, XeCl laser (mass density 1 gm/cc assumed) [64]; e, E - calcified plaque, dye laser [57]; F - kidney stone, dye laser [52].